IOSR Journal of Mechanical and Civil Engineering (IOSR-JMCE)
e-ISSN: 2278-1684,p-ISSN: 2320-334X, Volume 17, Issue 5 Ser. III (Sep. – Oct. 2020), PP 24-34
www.iosrjournals.org

Wind Tunnel Six Component Measurements on Delta Wing

SALAHELDIN H. OMAR
Professor of Aerospace and Autonomous Systems Engineering and former Chair; Talent and Technology Creativity Unit, University of Tabuk, Saudi Arabia.

SAAD A. Adam
Assistant Professor, Faculty of Engineering, University of Tobruk, Libya,

Abstract: *Vortex flow phenomena are always connected with high agility aircrafts with super maneuvering rates, slender body of revolutions, highly swept back and delta wings and others and have great impacts on their performance and safety. A comprehensive wind tunnel investigation has been accomplished on six component forces and moments measurements of a carbon-fiber delta wing at different angles of attack up to 73 degrees for a zero degree angle of sideslip. This Investigation has been carried out at two free stream velocities of 24m/s and 48 m/s to predict any effects of the Reynolds number on the acquired data. The effect of vortex initiation and breakdown on the acquired measurement data has been discussed.*

Keywords: *Vortex Flow, Vortex Breakdown, Vortex Dynamics, Delta Wing, Super Maneuvering Aircraft, High Agility Aircraft, Slender Body of Revolution, Wind Tunnel, six component balance, Data Acquisition System.*

Date of Submission: 5-10-2020 Date of Acceptance: 19-10-2020

Nomenclature

C local chord
Cp Surface pressure coefficient
Cr Wing root chord
h height over the leeward side
H Maximum wing profile thickness
r Radius of viscous subcore
k Number of waves
R Radial distance from the centre of the vortex core
Re Reynolds number based on chord length
S Local wing span
x Local chord-wise distance from wing apex
y Local span-wise distance from wing root
z Local distance above wing surface
Λ Aspect ratio
λ wave length
ρ Fluid density
ρo Reference density (a pure constant)
dt time step
Fx X component of the resultant pressure force
δ *Local vorticity thickness (vertical extent of mixing zone)*
Δρ Density difference of two adjacent fluid streams
ΔU Difference between flow Velocities of two adjacent fluid streams
ω Angular velocity
U∞ Free stream speed
Vaxial Vortex axial velocity
Vswirl Vortex swirl velocity
α *Wing angle of attack*
αc Vortex-core angle of attack
Λc Vortex-core sweep angle
β *Wing angle side slip*
ΛLE Wing sweep back angle
ϕ *Swirl angle = tan-1 (Vswirl / Vaxial)*

I. 1 Introduction

1.1. The Vortical flow over delta wings

Vortical flow is important phenomena associated with high agility aircrafts at super maneuvering, rates, slender body of revolutions, highly swept back wings and delta wing, dynamical meteorology covering Thunderstorms, Sea breeze, Tornado, Hurricane, Mountain waves, and physical oceanography including oceanic waves, vortices, currents, long oceanic waves, atmospheric convection, and natural oscillations in air-sea interactions. High agility aircrafts maneuvering at high angles of attack might be affected by Asymmetrical and antisymmetrical vortical flow and breakdown leading to large side forces and yawing moments beyond the maximum moments affordable by the control surfaces.

1.2. Vortices over delta wings;

In a homogeneous fluid, mixing requires enough energy necessary to overcome mechanical frictions, but in a stratified fluid additional energy is necessary to raise heavy fluid parcels and lower light fluid parcels against buoyancy forces increasing the potential energy and therefore the mixing can proceed spontaneously if the reduction in the kinetic-energy exceeds the increase in the potential-energy. Mixing of fluid parcels can be performed only if the initial density-difference is small enough to avoid an insurmountable gravitational barrier Thorpe, S. A. (1968, 1971), or if the initial velocity-shear is large enough to provide the necessary energy for the fluid mixing process to take place. The ratio between potential and kinetic energies has been defined as Richardson number "Ri", with the numerator is the potential-energy barrier that mixing process must overcome to be performed and the denominator is the available kinetic energy of the shear flow.

Richradson number = $(g/\rho_o)\ \Delta\rho\ \delta/\Delta U^2$ after Richardson Lewis Fry (1922)

Kelvin-Helmholtz instability was first studied by Taylor in 1915 (Taylor, G. I., (1931)). Summarizing that Richardson number must be less than ¼ for instability to take place, otherwise, the mixing process occurs only locally in a vicinity of the initial interface and will not therefore be able to spread over the whole system. The flow streamlines of both sides of delta wing join at the separation line along the wing leading edge forming separated free shear layer of two separated adjacent streams of different velocities, namely the lower velocity stream from the pressure side, and the higher velocity stream from the suction leeside. The different velocities of the two parallel streams of the separated shear layer initiate inviscid instability of a constant-vorticity layer in the interfacial region inside the free shear layer and generate laminar small waves which distorts the boundaries of the region containing the vorticities as in figure 1(a). The perturbations induce vertical velocities which force the perturbations and waves to grow into discrete vortices and therefore increasing the thickness of the free shear layer by moving away from the leading edge, figure 1 (b). These spatially growing mixing layers are characterized by the formation of big spiral vortices resulting from Kelvin-Helmholtz instability. Each vorticity tends to entrain the other neighbored vorticity under the influence of their induced velocity forcing both vortices to rotate around one another in pair due to the nonlinear interaction. Every vorticity rotate slower at its outer part than close to the center initiating tails as shown in figure 1-C which merge into spirals during the pairing Piercy N. A. V. (1923), Winant, C. et al (1974). The interfacial region of constant vorticity becomes periodically fatter and thinner, figure 1 (c) and the pairing process starts. The pairing process amplifies the spatial and irregularities in the vortex structure and increasing the variations in the length and strength of the vortical cores which are continually rotating around one another in pairs forming the rotating vortex lumps in the interfacial region of the free shear layer figure 1(d) and figure 2.

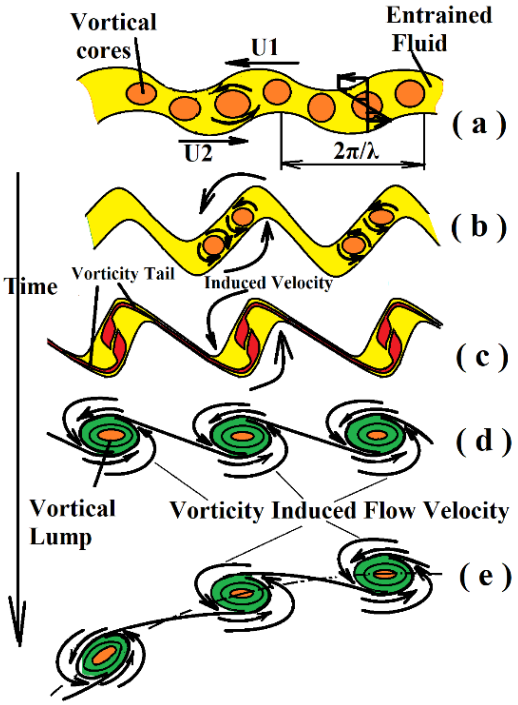

Figure 1 (a-e): Vortex pairing and lumps

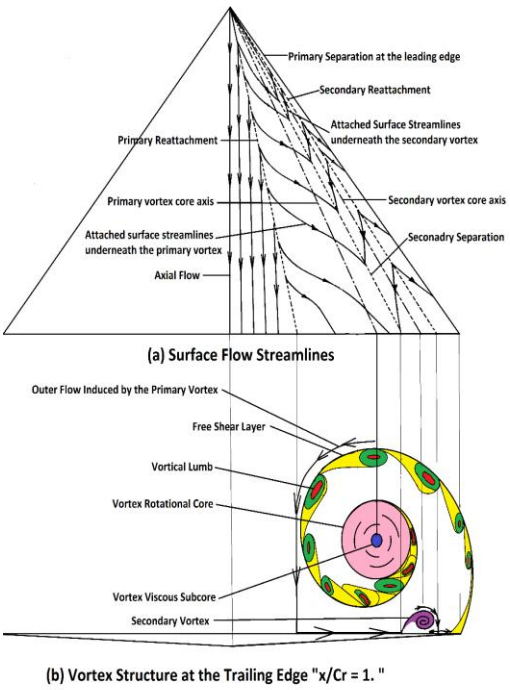

Figure 2: surface flow stream lines and vortical flow of a delta wing

The free shear layer rolls up into a vortex core by the impact of the vorticity induced flow velocities on both sides of vortical lumps within the free shear layer as shown in figure 1- (d and e), 2, and figure 3 of wind tunnel smoke and laser light sheet flow visualization over sharp edged delta wing after Omar Salaheldin H. (2020) [7]. The primary vortex can be divided, after [1] Earnshaw P. (1962), into three regions, namely; the free shear layer, the rotational core, and viscous subcore as shown in figure 2. The free shear layer generated at the leading edge rolled up forming the primary vortex induces the outer flow of the primary vortex to reattach on the leeward side of the delta wing and is continually providing the boundary layer after the reattachment line with fresh air of high energy as illustrated in figure 2. The reattached flow moves from the reattachment line outboard toward the leading edge until it separates at the secondary separation line somewhere between the axis of the primary vortex and the leading edge in dependence of the flow condition "laminar/turbulent" forming the secondary vortex which which affects the surface pressure on the leeward side of the wing Omar Salaheldin H. (2020) [6]. Tertiary vortex may be initiated underneath the secondary vortex with a rotation in the same sense of the primary vortex having its effect on the surface pressure of the leeward side of the wing Omar Salaheldin H. (2020) [6].

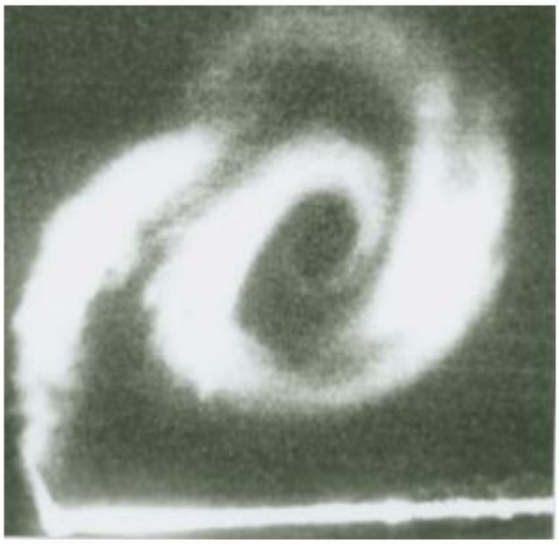

Figure 3: Laser smoke and light sheet illumination of the cross flow on a sharp edged delta wing, after Omar, Salaheldin H (2020) [7].

1.3 Vortex Breakdown

Vortex breakdown is defined by Sarpkaya T. (1971) as an abrupt change in the structure of the vortex core, followed by a growing asymmetric flow around the vortex axis. Leibovich S. (1978), and [2] Garg A., Leibovich S. (1979) defined vortex breakdown as a disturbance that is characterized by the formation of an internal stagnation point on the vortex axis followed by a reversed flow. Vortex breakdown has many different and contradictory aspects of view and interpretations. Vortex breakdown occurs, after [3] Hall, M. (1972), in dependence of the magnitude of the flow swirling, as an indication of the vorticity shedded in the rolled up free shear layer, and of the external pressure gradient and the degree of the divergence as indication of the vorticity convection along the vortex axis [5] Michalke, A. (1962). At a certain angle of attack the increased rate of generation of the vortices shedded in the vortex sheet exceeds the convection of these vortices leading to an increase in the concentrated vortices, which have limits on the their maximum amount of vortices per unit area "critical vortices concentration". By exceeding these limits, the shedded vortices in the rolled up free shear layer cannot be compensated by the convection of the vortices, which is dependent on the increased component of the axial flow velocity by increasing the angle of attack, and gradually, the axial momentum becomes too weak to overcome the adverse pressure gradient, leading to a drastic increase in the interactions among the vortex-outer-core spirals, and to the formation of a stagnation point along the viscous subcore, subsequently, the vortex cannot maintain its organized structure leading to a spiral form or bubble form vortex breakdown, as in figure 4, spreading the vortices over a wider region and the excessive vortices are redistributed in the region aft the vortex breakdown location reducing the vorticity concentration inside the vortical sheet. This phenomenon have been observed during the flow visualization using smoke/laser light sheet technique in wind tunnel at 40 degree angle of attack after Omar Salaheldin H. (2020) [7]. More details are available in the Review of Omar, Salaheldin H. (2020) [5].

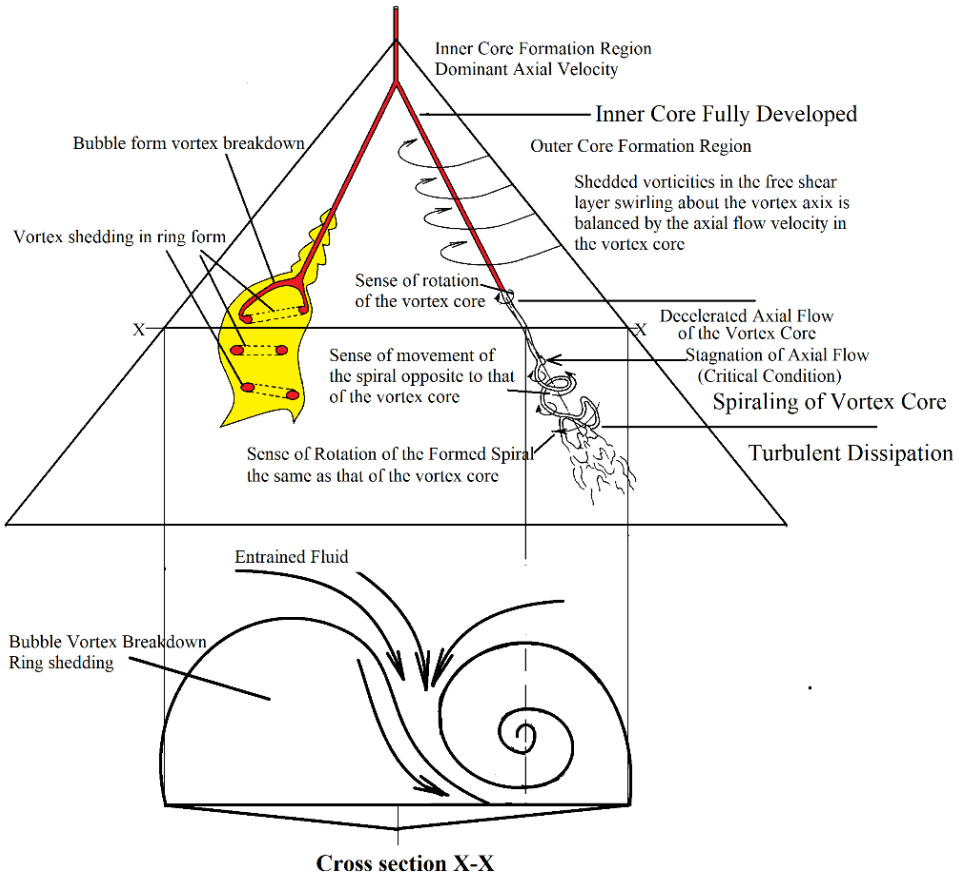

Figure 4: Vortex formation and breakdown over delta wings

II. Experimental Setup

2.1. Wind tunnel facility and test condition

All experiments were carried out in a low speed closed loop water cooled wind tunnel of TU Munich. The test section of the wind tunnel is an open flow test section of 1.2 meter diameter, 72 m/s maximum speed, and 0.2-0.3 % turbulence as shown in figure 5 a-d.

(a) (b) (c)

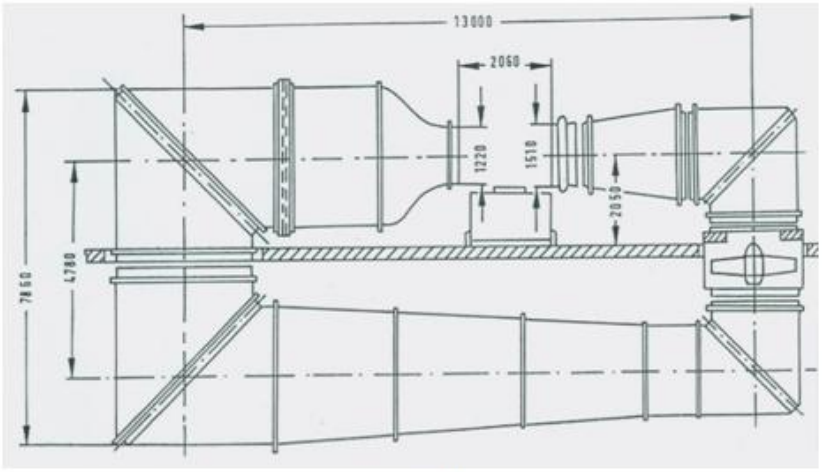

(d)

Figure 5: Wind Tunnel Facility and test model

2.2. Wind Tunnel Test Model

The wind tunnel test model is a sharp edged delta wing manufactured from carbon fibers to predict solely the aerodynamic forces by minimizing elastic forces and inertia forces, which interact mutually with the aerodynamic forces changing their predicted values. The development and breakdown of the vortex over the leeside of the delta wing as well as the vortex shedding at very high angles of attack up to 65^{O} have been predicted.

The test model is a light weight, stiff, sharp edged delta wing made from carbon fibers of aspect ratio Λ =1, sweep back angle Λ_{LE} of 76^{O}, length of 670mm, chord of 335mm and maximum thickness h of 57mm as shown in figure 6.

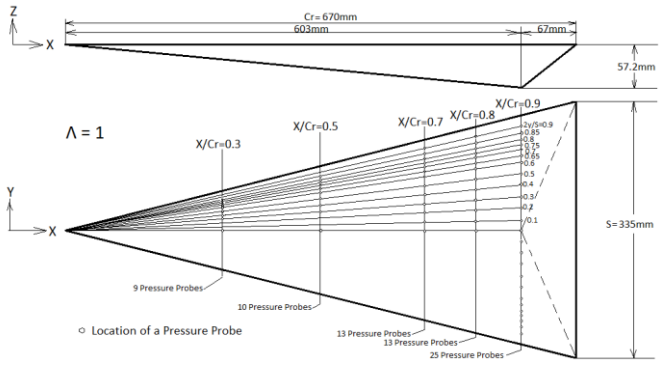

Figure 6 Delta wing dimension

2.3. Six component balance and test procedure

Forces and moments acting on the delta model were predicted using six component balance from the company PFISTER (figure 5-a), which could predict directly and simultaneously lift, drag, and lateral forces as well as nose-down pitching, yaw, and roll moments. The balance support (figure 5 a, b) is fixed on a hydrostatic suspended balance plate, which measures 10 values for each component per second (10 Hz sampling rate) and averaging the measured signals during one minute displaying all c components on 6 digital screens and the PC monitor and store the acquired data on the hard disk of the PC (figure 7-c).

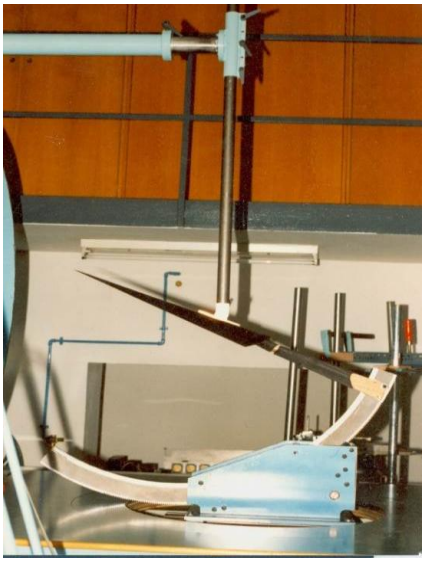

Figure 7-a: The delta wing separated from the support of the 6-component balance and fixed instead to upper support

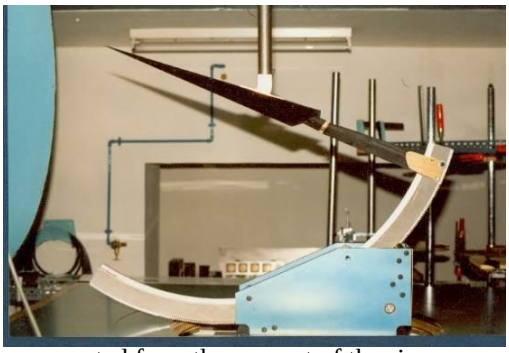

Figure 7-b: The delta wing separated from the support of the six component balance and fixed to upper support

Figure 7-c the six component balance data acquisition system and the speed control system of the wind tunnel

All measurements are carried out twice, the first measurement is executed with the wing test model fixed to the support of the balance measuring all six components (forces and moments) acting on the test model and on the balance support together (figure 5 a, b, d), while the second test is accomplished with the test model fixed to an upper vertical support fixed to the wind tunnel upper side to measure the six component forces and moments acting only on the support of the balance separated from the test model (figure 7 a, b) . The second measurement is necessary to cancel the measured forces and moments acting on the balance support alone and get therefore the forces and moments acting on the delta test model alone by calculating the difference of the forces and moments from both measurements.

III. Results And Discussions

At zero angle of attack all predicted forces and moments are close to zero (figures 8-13). The already initiated leading-edge vortex at this angle of attack is too weak and the cross flow over the lee-ward side of the wing represents a considerable velocity component leading to deviations mainly in the lift force Cl and side force Cy from the zero-value (figure 8, 10). The "negative" side force Cy (figure 10) increased slightly with the angle of attack up to 5 degrees due to the same reasons mentioned before, but it decreased again to reach an average of zero at 15 degrees and a local maximum "positive" value at 20 degrees is predicted, at which the effect of the laminar turbulent transition of the boundary layer results in a drastic change of the predicted values in the opposite direction "negative" and the negative values increased with the angle of attack up to 30 degrees. The Reynolds effect on the predicted values of the side force Cy at 20 degrees angle of attack is significant. This effect seems to be due to the laminar/turbulent transition at the high free stream speed of 48 m/s and the increased magnification time of the disturbances inside the rolled-up free shear layer.

The lift Cl, lift induced drag Cd and nose-down pitch moment Cn increase nonlinearly with the angle of attack up to 10 to 20 degrees (figures 8, 9, 12). At angle of attack up to 10 degrees there is no significant change in the roll Cr and yaw Cn moments, but they increase nonlinearly from 10 to 20 degrees.

The acquired data of the forces and moments indicate that roll moment Cr is influenced directly by lift and drag, while yaw moment by drag and side force. By increasing the angle of attack up to 30 degrees the lift Cl, drag Cd, negative side force Cy and, subsequently, the nose-down pitch Cm, yaw Cn, and roll Cr moments increase drastically to reach local maximums at about 30 degrees angle of attack, at which the bursting location of the leading-edge vortex lies closer to the trailing edge at X/C = 1.15 and has together with the increased back-flow over the rear part of the wing and the down vortex a significant effect on the forces and moments of the delta wing (figures 8-13). These effects together with the upstream movement of the vortex bursting location over the wing, which reaches the trailing edge at about 31 degrees angle of attack, result in a significant decrease in the lift Cl, lift induced drag Cd, pitch Cm and roll Cr moments by increasing the angle of attack up to 35 degrees (figures 8, 9, 11, 13). At this angle of attack the vortex bursting location lies at X/C = 0.5 over the wing far from the region of strong adverse pressure gradients downstream to the trailing edge, the back-flow region in the rear part of the wing and from the down vortex leading to damping their effects on the upstream movement of the bursting location and a slight increase of the lift and nose-down pitch moment and drastic increase of the drag force and roll moment are predicted. The drastic increase of the drag Cd and roll moment Cr are mainly due to the existence of different types and locations of the vortex breakdown over each side of the wing, which are predicted at 40 degrees angle of attack (figures 9, 13).

It is to be mentioned that simultaneous vortex shedding start in the range of 35 to 37 degrees and up to 70 to 90 degrees angle of attack leading to increasing the drag Cd and affecting all other components of forces and moments (figures 8-13). By increasing the angle of attack over 40 degrees all forces and moments decrease drastically up to about 50 degrees for the side force and yaw moment and 60 degrees for the lift Cl, lift induced drag Cd, nose-down pitch Cm and roll moments Cr. At 60 degrees angle of attack the vortex bursting location reached its maximum upstream position over the wing leading to a slight increase in the lift Cl and nose-down pitch moment Cm up to about 65 degrees followed a drastic decrease in the side force and yaw and roll moments up to about 70 to 85 degrees. The drag force Cd increases significantly at angles of attack over 65 degrees due to the increased intensity of the shedded vortices. These results are well correlated with the surface pressure distribution on the leeward side of the wing Omar Salaheldin H. (2020) [5] and the Flow visualization using liquid crystals and laser light sheet/smoke Omar Salaheldin H. (2020) [6].

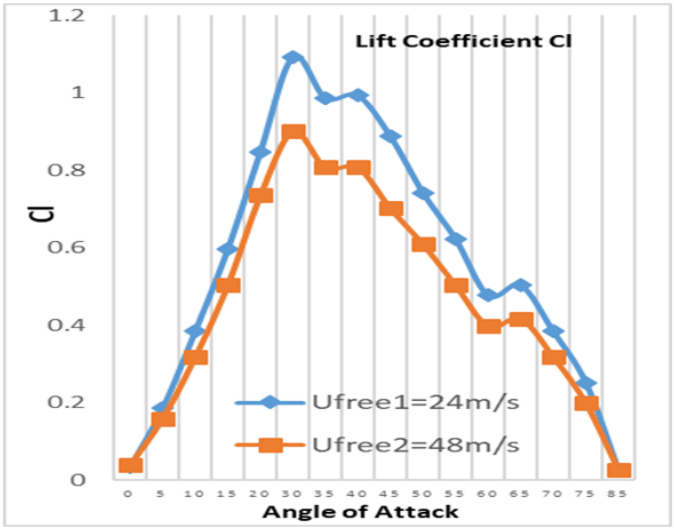

Figure 8 Cl

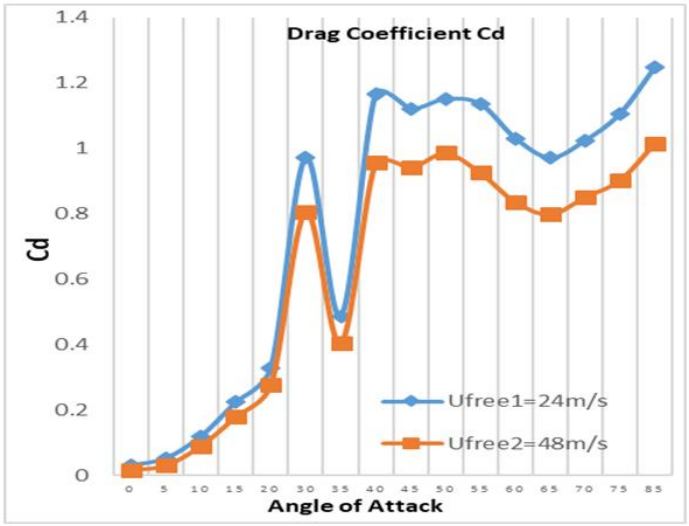

Figure 9 Cd

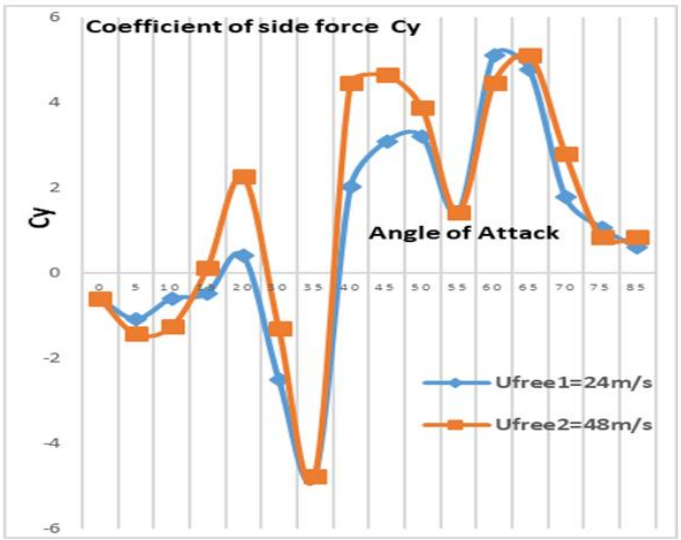

Figure 10 Cy

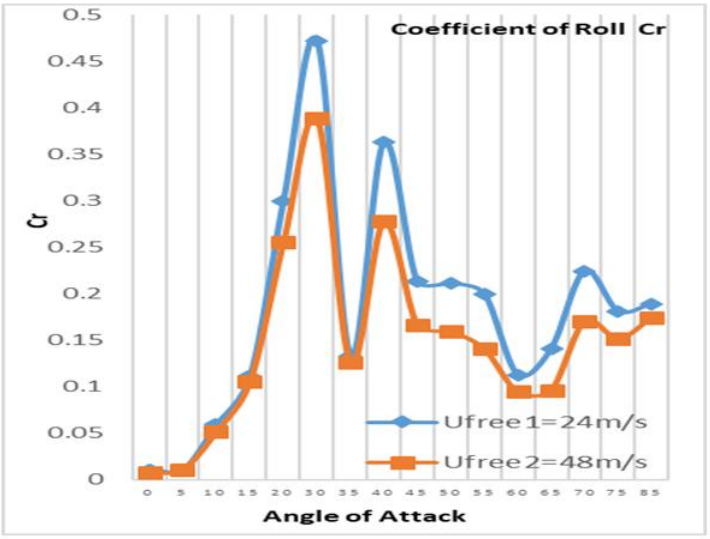

Figure 11 Cm

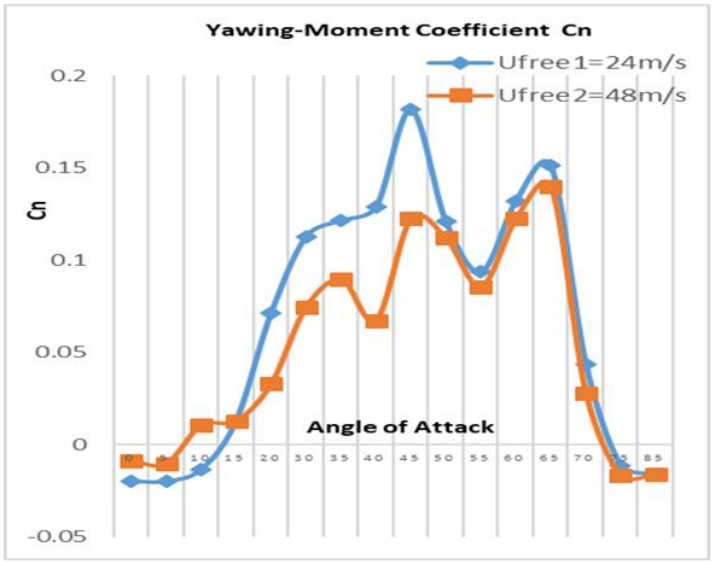

Figure 12 Cn

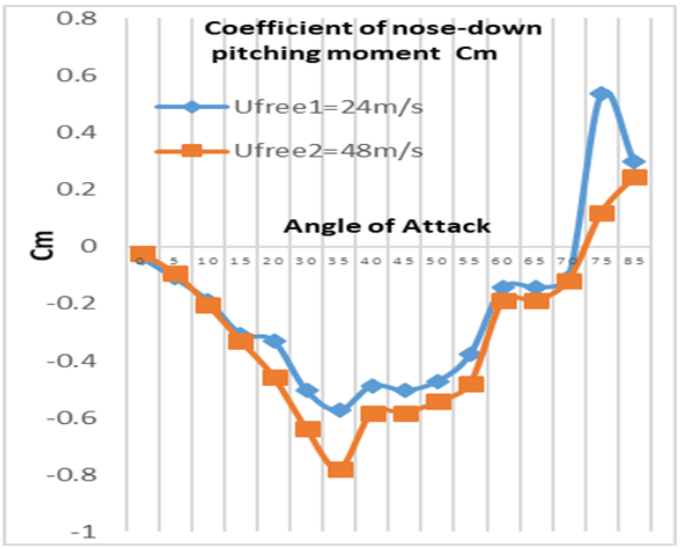

Figure 13 Cr

IV. Summary

In this part of the investigation (Part IV), six component force and moment measurements have been carried out at different angles of attack from zero up to 85 degree for two free stream wind tunnel speeds of 24m/s and 48m/s.

At zero angle of attack all predicted forces and moments are close to zero. The already initiated leading-edge vortex at this angle of attack is too weak and the cross flow over the lee-ward side of the wing represents a considerable velocity component leading to measurable values mainly in the lift force Cl and side force Cy. The "negative" side force Cy increased slightly with the angle of attack up to 5 degrees due to the same reasons mentioned before, but it decreased again to reach an average of zero at 15 degrees and a local maximum "positive" value at 20 degrees is predicted, at which the effect of the laminar turbulent transition of the boundary layer results in a drastic change of the predicted values in the opposite direction "negative" and the negative values increased with the angle of attack up to 30 degrees. The Reynolds effect on the predicted values of the side force Cy at 20 degrees angle of attack is significant. This effect seems to be due to the laminar/turbulent transition at the high free stream speed of 48 m/s and the increased magnification time of the disturbances inside the rolled-up free shear layer.

The lift Cl, lift induced drag Cd and nose-down pitch moment Cn increase nonlinearly with the angle of attack up to 10 to 20 degrees. At angle of attack up to 10 degrees there is no significant change in the roll Cr and yaw Cn moments, but they increase nonlinearly from 10 to 20 degrees.

The acquired data of the forces and moments indicate that roll moment Cr is influenced directly by lift and drag, while yaw moment by drag and side force. By increasing the angle of attack up to 30 degrees the lift Cl, drag Cd, negative side force Cy and, subsequently, the nose-down pitch Cm, yaw Cn, and roll Cr moments increase drastically to reach local maximums at about 30 degrees angle of attack, at which the bursting location of the leading-edge vortex lies closer to the trailing edge at X/C = 1.15 and has together with the increased back-flow over the rear part of the wing and the down vortex a significant effect on the forces and moments of the delta wing. These effects together with the upstream movement of the vortex bursting location over the wing, which reaches the trailing edge at about 31 degrees angle of attack, result in a significant decrease in the lift Cl, lift induced drag Cd, pitch Cm and roll Cr moments by increasing the angle of attack up to 35 degrees. At this angle of attack the vortex bursting location lies at X/C = 0.5 over the wing far from the region of strong adverse pressure gradients downstream to the trailing edge, the back-flow region in the rear part of the wing and from the down vortex leading to damping their effects on the upstream movement of the bursting location and a slight increase of the lift and nose-down pitch moment and drastic increase of the drag force and roll moment are predicted. The drastic increase of the drag Cd and roll moment Cr are mainly due to the existence of different types and locations of the vortex breakdown over each side of the wing, which are predicted at 40 degrees angle of attack.

It is to be mentioned that simultaneous vortex shedding start in the range of 35 to 37 degrees and up to 70 to 90 degrees angle of attack leading to increasing the drag Cd and affecting all other components of forces and moments. By increasing the angle of attack over 40 degrees all forces and moments decrease drastically up to about 50 degrees for the side force and yaw moment and 60 degrees for the lift Cl, lift induced drag Cd, nose-down pitch Cm and roll moments Cr. At 60 degrees angle of attack the vortex bursting location reached its maximum upstream position over the wing leading to a slight increase in the lift Cl and nose-down pitch moment Cm up to about 65 degrees followed a drastic decrease in the side force and yaw and roll moments up to about 70 to 85 degrees. The drag force Cd increases significantly at angles of attack over 65 degrees due to the increased intensity of the shedded vortices.

References

[1]. Earnshaw, P. B (1962). An experimental investigation of the structure of a leading edge vortex. ARC R & M 3281, 1962.

[2]. Garg, A.K.; Leibovich, S. (1979). Spectral Characteristics of Vortex Breakdown Flow Fields, Physics of Fluids, Vol. 22, No. 11, 1979, pp. 2053-2064. Unsteady Aspects of Leading-edge Vortices RTO-TR-AVT-080 6 -33

[3]. Hall, M.G. (1972). Vortex breakdown. Ann. Rev. Fluid Mech. 4, 195-218 (1972)

[4]. Leibovich S. (1979). The structure of vortex breakdown, Annual Review Fluid Mech. 10, 221 (1978).

[5]. Michalke, A. (1965). Vortex formation in a free boundary layer according to stability theory, J. Fluid Mech. (1965), vol. 22, part 2, pp. 371-383.

[6]. Omar Salaheldin H. (2020); A REVIEW ON VORTEX FLOW OVER DELTA WINGS AT HIGH ANGLES OF ATTACK, International Journal Of Core Engineering & Management International Journal Of Core Engineering & Management Volume-6, Issue-9, 2020. http://ijcem.in/archive/volume-6-issue-9-2020-current-issue/

[7]. Omar Salaheldin H. (2020); WIND TUNNEL INVESTIGATION ON SURFACE-PRESSURESAND VORTEX FLOWOVER DELTA WING AT HIGH ANGLES OF ATTACK AND FREE-STREAM VELOCITIES International Journal Of Core Engineering & Management Volume-6, Issue-8, 2020. http://ijcem.in/archive/volume-6-issue-8-2020-current-issue/

[8]. Omar Salaheldin H. et al.(2020); WIND TUNNEL VORTEX FLOW VISUALIZATION AND TRACKING ON A DELTA WING AT HIGH ANGLES OF ATTACK, International Journal Of Core Engineering & Management Volume-6, Issue-7, 2020. http://ijcem.in/archive/volume-6-issue-7-2020-current-issue/

[9]. Piercy N.A.V. (1923). On the vortex pair quickly formed by some aerofoils, J. R. Aeronaut. Soc. 27 488–500.

[10].] Sarpkaya, T. (1971). Vortex Breakdown in Swirling Conical Flows, in: AIAA Journal, pp 1792-1799, Vol. 9, No. 9, April 1971.

[11]. Richardson Lewis Fry (1922). Weather Prediction by Numerical Process, Second Edition, Cambridge University Press, ISBN: 0-521-68044-1 (250pp)
[12]. Taylor, G. I., (1931). Effect of variation in density on the stability of superposed streams of fluid. Proc. R. Soc. London A, 132, 499–523.
[13]. Thorpe, S. A. 1968 A method of producing a shear-flow in a stratified fluid. J. Fluid Mech. 32, 693-704.
[14]. Thorpe, S. A. (1971). Journal of Fluid Mechanics 46: 299{319 (1971).
[15]. Winant, C. D.; Browand, F. K. (1974). Vortex Pairing: The Mechanism of Turbulent Mixing-Layer Growth at Moderate Reynolds Number, in: Journal of Fluid Mechanics, pp 237-255, Vol. 63, Part 2, 1974.

SALAHELDIN H. OMAR, et. al. "Wind Tunnel Six Component Measurements on Delta Wing." *IOSR Journal of Mechanical and Civil Engineering (IOSR-JMCE)*, 17(5), 2020, pp. 24-34.